POTGIETER, J.H., SKINNER, W., and HEYNS, A.M. Influence of ruthenium content on the corrosion in sulphuric acid of a duplex stainless steel. *INFACON 6. Proceedings of the 1st International Chromium Steel and Alloys Congress, Cape Town.* Volume 2. Johannesburg, SAIMM, 1992. pp. 235–240.

Influence of Ruthenium Content on the Corrosion in Sulphuric Acid of a Duplex Stainless Steel

J.H. POTGIETER*, W. SKINNER†, and A.M. HEYNS†
**Mintek, Randburg, South Africa*
†University of Pretoria, Pretoria, South Africa

The influence of the ruthenium content in a 22%Cr duplex stainless steel on the corrosion rate of the alloy in sulphuric acid was investigated by means of mass-loss tests and electrochemical measurements. Characteristic trends were determined from mass-loss tests by the construction of graphs of corrosion rate as a function of the ruthenium content for different concentrations of sulphuric acid at different temperatures. Before the potentiodynamic measurements were carried out, the determinations of linear polarization resistance were used to establish when steady-state conditions were reached in each investigation.

In this paper, the corrosion rates obtained by the different techniques are compared, and the characteristic electrochemical parameters in each case are summarized. The corrosion behaviour is explained by the use of Evans diagrams. It is concluded that ruthenium increased the corrosion resistance of the alloys investigated by inhibiting the anodic-dissolution reaction.

Introduction

Some stainless-steel alloys that contain small additions of platinum-group metals (PGMs) have a remarkable corrosion resistance in reducing acid media[1-3]. The introduction of active cathodes into the alloy results in a lowering of the hydrogen over-potential. This increases the ability of the alloy to passivate. The technique is known as cathodic modification[4].

Although several investigations have been carried out on the corrosion behaviour of cathodically modified ferritic and austenitic stainless steels in reducing acid media, very little is known about the behaviour of duplex stainless steels in such media[3]. Limited previous work has indicated that the behaviour of duplex stainless steels is slightly different from that of pure austenitic and ferritic stainless steels, although no thorough explanation of the role of different phases and partitioning effects is given. The purpose of this paper is therefore to characterize the corrosion behaviour in sulphuric acid of a duplex stainless steel containing 22 per cent chromium and different concentrations of ruthenium (0 to 0,3% Ru).

The reason why ruthenium was chosen as the additive is mainly for economic reasons. Ruthenium is the cheapest of the PGMs, and would thus increase the price of the final alloy less than any of the other PGMs would.

Experimental

Materials

The alloys used in this investigation were melted in a vacuum induction furnace, and rectangular ingots of approximately 45 by 70 by 170 mm, with a mass of between 3 and 5 kg each, were produced. Chemical analyses of the alloys are shown in Table I. Since no deliberate nitrogen additions were made, it was necessary to increase the nickel contents of these alloys to 9 per cent, as compared with tbe 5,5 per cent in commercial duplex alloys, so that an alloy consisting of approximately equal amounts of ferrite and austenite could be obtained.

Each ingot was hot-rolled to a plate with a thickness of between 3 and 6 mm. These hot-rolled plates were solution-annealed for 1 hour at 1060 °C to produce duplex alloys containing approximately 50 per cent austenite and 50 per cent ferrite. The plates were quenched after rolling and heat

TABLE I
CHEMICAL COMPOSITION OF THE MATERIALS STUDIED IN PERCENTAGES BY MASS*

Alloy	Target composition	Cr	Ni	Mo	Ru	Mn	Si	S	P	O	N	C
2209A	Fe–22%Cr–9%NI–3%Mo–0%Ru	22,0	9,07	2,81	–	0,1	0,070	0,01	0,01	0,021	0,006	0,03
2209B	Fe–22%Cr–9%Ni–3%Mo–0,1%Ru	22,1	9,20	2,89	0,14	0,1	0,025	0,01	0,01	0,042	0,006	0,03
2209C	Fe–22%Cr–9%Ni–3%Mo–0,2%Ru	22,4	9,14	2,82	0,22	0,1	0,030	0,01	0,01	0,050	0,004	0,03
2209D	Fe–22%Cr–9%Ni–3%Mo–0,3%Ru	22,4	9,24	2,92	0,28	0,1	0,030	0,01	0,01	0,037	0,005	0,02

* The balance of the alloys was Fe

treatment to prevent the occurrence of 475 °C embrittlement and sigma-phase formation. Further experimental details are available elsewhere[5].

Immersion Tests

Mass-loss tests to determine the corrosion rates at different temperatures and acid concentrations were carried out according to ASTM standards[6]. Specimens of approximately 2,5 to 3,0 cm by 2,5 to 3,0 cm by 0,3 to 0,5 cm were cut from each annealed alloy and polished to a 120-grit finish. The specimens were then rinsed in distilled water and isopropanol, and their masses and dimensions were measured.

Corrosion tests were carried out at three different temperatures (25, 55, and 90 °C) using a 2,0 dm^3 cylindrical glass vessel fitted with a water-cooled Allihn drip-tip condenser. Exposure times varied from 30 minutes to 48 hours. Approximately 0,9 dm^3 of solution was used for each specimen. All the solutions were de-aerated with high-purity nitrogen for at least 30 minutes before each test was carried out, as well as during the test, except in the tests conducted at temperatures of 90 °C. The specimens were held in an open glass cradle to permit free circulation of the acid solution. After 30 minutes to 48 hours of immersion, the specimens were removed, cleaned mechanically with a nylon hairbrush, rinsed in demineralized water and isopropanol, dried, and their masses determined. The physical characteristics of the steels investigated are summarized in Table II.

The corrosion rates calculated from the mass-loss tests for each of the different alloys are summarized in Table III.

TABLE II
PHYSICAL CHARACTERISTICS OF 22 PER CENT CHROMIUM DUPLEX STAINLESS STEELS

Alloy	Density g/cm^3	Equivalent mass[7]	Ferrite grain size µm
Fe–22%Cr–9%Ni–3%Mo–0%Ru	7,64±0,11	25,31	6,10
Fe–22%Cr–9%Ni–3%Mo–0,14%Ru	7,64±0,09	25,27	5,90
Fe–22%Cr–9%Ni–3%Mo–0,22%Ru	7,64±0,10	25,22	5,70
Fe–22%Cr–9%Ni–3%Mo–0,28%Ru	7,64±0,10	25,20	6,10

Electrochemical Measurements

Polarization measurements were carried out according to ASTM standards[6]. Disk test specimens 15 mm in diameter were spark-eroded from each plate, polished to a surface finish of 1 µm on a diamond cloth, and cleaned in isopropanol before use. A glass cell was used, with five bottlenecks housing the working electrode, a saturated-calomel reference electrode, two graphite counter-electrodes, and a nitrogen purger. Tests were conducted in various sulphuric acid solutions. Before each run, the solution was purged with high-putity nitrogen for at least 30 minutes.

Polarization-resistance measurements, as well as potentiodynamic scans, were carried out with a Solartron potentiostat. The polarization-resistance scans were performed from –30 mV versus E_{corr} to +30 mV versus E_{corr}. A scan rate of 0,1 mV/s was employed, and scans were carried out at various time intervals. No *IR*-compensation was done, since all the solutions were highly conducting.

Before the potentiodynamic scans, graphs of $1/R_p$ versus time were constructed to determine the time required by the system to reach steady-state conditions. For alloy/electrolyte systems stabilizing at a relatively electropositive corrosion potential (indicating passivation control), the anodic potentiodynamic scans were carried out first, and cathodic potentiodynamic scans were done after a retum to steady-state conditions. For alloy/electrolyte systems stabilizing at a relatively electronegative corrosion potential (indicating activation control), the cathodic potentiodynamic scans were done first, followed by the anodic potentiodynamic scans when steady-state conditions had been reached – 15 to 30 minutes later The cathodic potentiodynamic responses were recorded, starting at the open-circuit corrosion potential to –200 mV versus E_{corr}. Anodic potentiodynamic scans were started at the open-circuit corrosion potential, and continued to approximately +1200 mV versus E_{corr}. The scan rates for both the anodic and the cathodic potentiodynamic scans were 0,2 mV/s.

The temperature was controlled by use of a waterbath, and was constant to 1 °C from the set temperature.

TABLE III
CORROSION RATES (mm/a) OF 22% Cr DUPLEX STAINLESS STEELS IN H_2SO_4

Temp. °C	Immersion time h	H_2SO_4 %	22%Cr–9%Ni–3%Mo alloy with			
			0% Ru	0,14% Ru	0,22% Ru	0,28% Ru
25	48	1	0,0000	0,0000	0,0000	0,0000
25	48	10	0,0040	0,0040	0,0052	0,0000
25	48	20	0,0056	0,0058	0,0034	0,0000
25	48	30	0,0063	0,0070	0,0078	0,0000
25	48	40	0,0084	0,0153	0,0156	0,0000
55	48	1	0,0036	0,0043	0,0043	0,0000
55	48	10	0,0056	0,0068	0,0043	0,0000
55	48	20	0,0409	0,0144	0,0125	0,0000
55	48	30	0,4929	0,0147	0,0318	0,0000
55	48	40	70,12	0,1250	0,1479	0,0000
90	0,5	1	0,1347	0,1250	0,1479	0,0000
90	0,5	10	3,155	0,5723	0,4085	0,0000
90	0,5	20	154,1	2,877	2,129	1,278
90	0,5	30	474,1	24,73	4,147	2,481
90	0,5	40	741,0	75,80	36,33	26,70

Results and Discussion

The results obtained from the immersion tests, which are summarized in Table III, were used in the construction of graphs of corrosion rate as a function of ruthenium content at specific temperatures and acid concentrations (Figures 1 to 3).

Figure l(a) shows no corrosion occurring in all four alloys, indicating that they are all under passivation control. Figures l(b) to (e) depict similar corrosion rates for all the alloys, except the one containing most ruthenium (0,28 per cent). Furthermore, these corrosion rates are very low, namely 20 µm /a or less. Figures 2(a) and (b) showed similar behaviour to that observed in Figures l(b) to (e). In Figures 2(c) and (d), there is a decreasing trend in the corrosion rate with increasing ruthenium content, but all the corrosion rates are still low. In this instance, the maximum corrosion rate (that of the alloy without any ruthenium) is still less than 50 µm/a. In the case of Figure 2(e), there is an abrupt decrease in the corrosion rate with the addition of ruthenium. The corrosion rates recorded are very high for the alloy without ruthenium, but still fairly low for the alloys with ruthenium, although much higher than previously observed. The same trend is also displayed in Figures 3(b) to (e).

Some of these behaviour patterns were investigated and charactenzed by means of further electrochemical measurements.

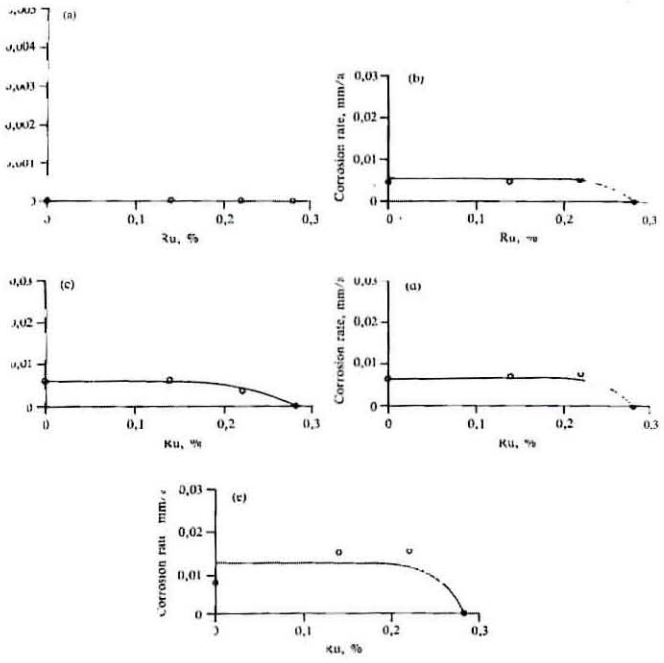

FIGURE 1. Corrosion rates of a 22% Cr duplex stainless steel with varying ruthenium contents in different sulphuric acid solutions at 25 °C.
(a) 1% (b) 10% (c) 20% (d) 30% (e) 40% H_2SO_4

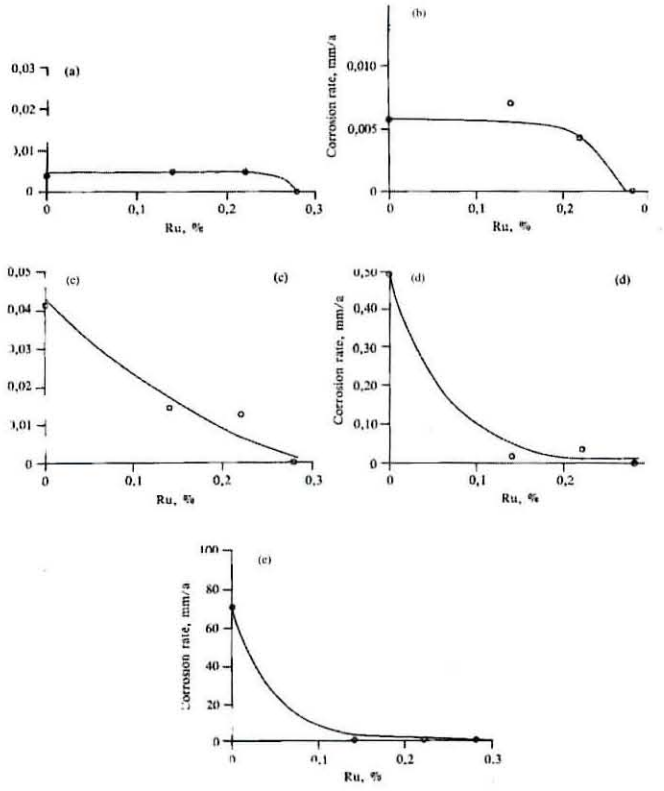

FIGURE 2. Corrosion rates of a 22% Cr duplex stainless steel with varying ruthenium contents in different sulphuric acid solutions at 55 °C.
(a) 1% (b) 10% (c) 20% (d) 30% (e) 40% H_2SO_4

It is clear from Figure 4 that in 10% H_2SO_4 at 55 °C the two alloys containing 0,22 and 0,28 per cent ruthenium exhibited spontaneous passivation, with the potentials all stabilizing at high noble values. The alloy without any ruthenium, as well as the one containing the least ruthenium, was in a state of active dissolution, with corresponding negative potentials. The respective passivation and activation control is supported by the potentiodynamic responses of all the alloys, as shown in Figure 5. Figure 6 shows the corresponding inverse polarization-resistance values against time for the same alloys. Inverse R_p values seem to decrease with increasing ruthenium content, corresponding to a decrease in corrosion rate as the ruthenium contents of the alloys increase. In all cases, it seemed as though steady-state conditions were reached not later than 20 hours after the exposure to the acid solution started.

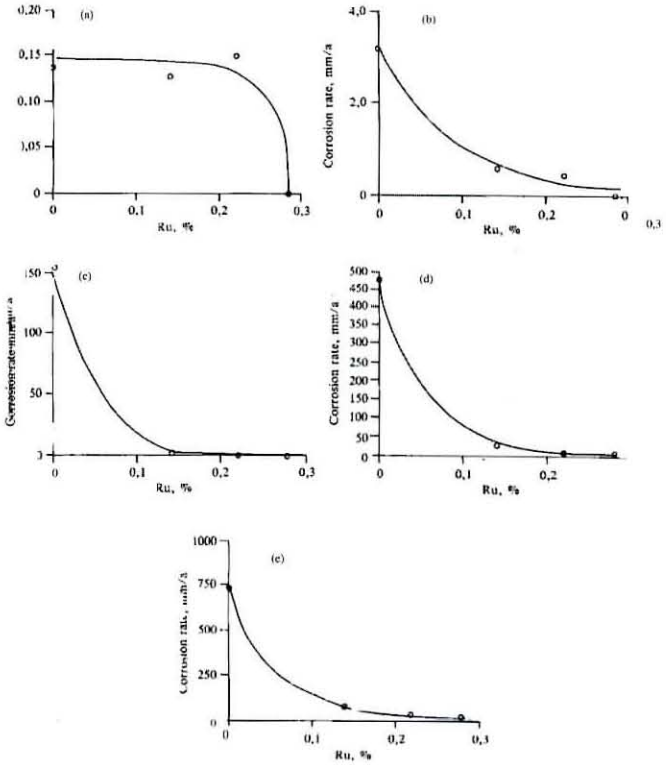

FIGURE 3. Corrosion rates of a 22% Cr duplex stainless steel with varying ruthenium contents in different sulphuric acid solutions at 90 °C.
(a) 1% (b) 10% (c) 20% (d) 30% (e) 40% H_2SO_4

Figure 7 summarizes the open-circuit potential versus time responses for the four alloys in a 20 per cent sulphuric acid solution at 55 °C. Again, the alloys containing 0 and 0,14 per cent ruthenium showed no sign of spontaneous passivation, and remained at relatively large electronegative potential values, which corresponds to activation control. The alloy containing 0,22 per cent ruthenium briefly achieved unstable passivation before stabilizing at electronegative potentials and remained activation controlled. Only the alloy containing 0,28 per cent ruthenium stabilized at a positive potential, indicating passivation control. The anodic potentiodynamic scans for these four alloys are presented in Figure 8, which clearly shows active–passive transition behaviour for all the specimens, except the alloy containing 0,28 per cent ruthenium, which is in the passive state.

From Figures 9(a) to (d), it seems as if the time required to reach steady-state conditions in the 20 per cent sulphuric acid solution is more or less 40 hours, which is about twice the time required in the 10 per cent sulphuric acid solution.

The $1/R_p$ values in the graphs in Figure 9 are also generally larger than for the alloys in 10 per cent sulphuric acid at 55 °C. Together with the previous observation, this would imply higher corrosion rates in the 20 per cent solution than in the 10 per cent solution, as is confirmed from a compari-

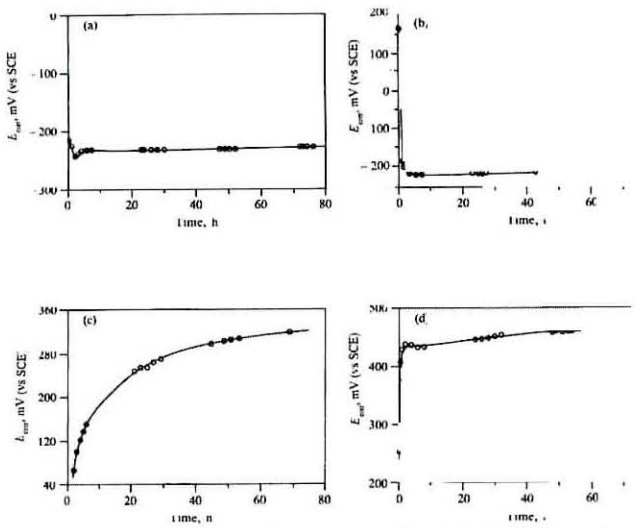

FIGURE 4. Potential versus time responses for a 22% Cr duplex stainless steel with varying ruthenium contents in a 10% sulphuric-acid solution at 55 °C. (a) 0% (b) 0.14% (c) 0,22% (d) 0,28% Ru

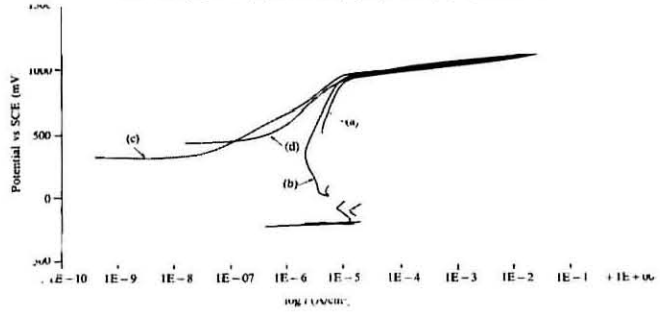

FIGURE 5. Anodic polarization curves for a 22% Cr duplex stainless steel with varying ruthenium contents in a 10% sulphuric acid solution at 55 °C. (a) 0% (b) 0,14% (c) 0,22% (d) 0,28% Ru

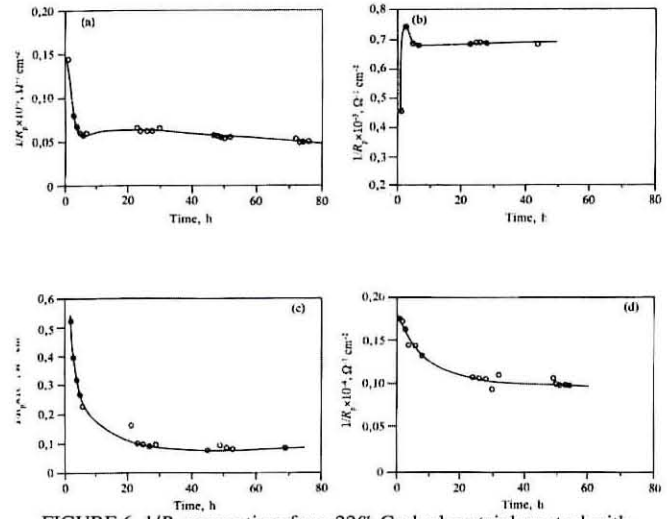

FIGURE 6. $1/R_p$ versus time for a 22% Cr duplex stainless steel with varying ruthenium contents in a 10% sulphuric acid solution at 55 °C. (a) 0% (b) 0,14% (c) 0,22% (d) 0,28% Ru

son of the mass-loss data in Table III. The values of $1/R_p$ in the graphs in Figure 9 also decrease from (a) to (d)– in other words, from the alloy without any ruthenium to the one with 0,28 per cent ruthenium, which corresponds to a decreasing corrosion rate with increasing ruthenium content

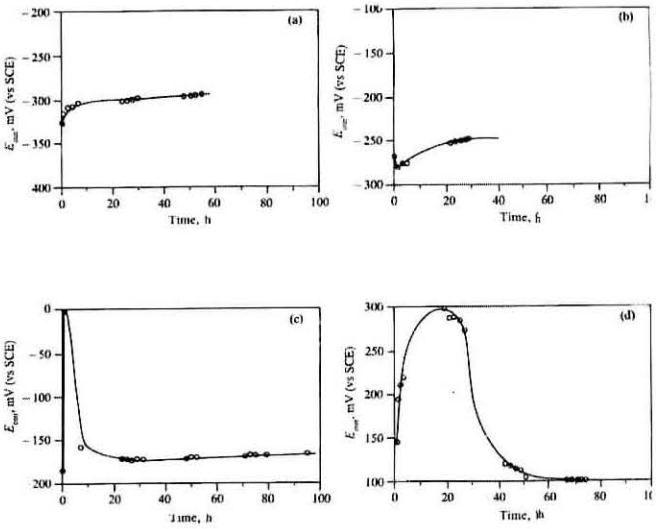

FIGURE 7. Open-circuit potential versus time responses for a 22% Cr duplex stainless steel with varying ruthenium contents in 20% H_2SO_4 at 55 °C. (a) 0% (b) 0,14% (c) 0,22% (d) 0,28% Ru

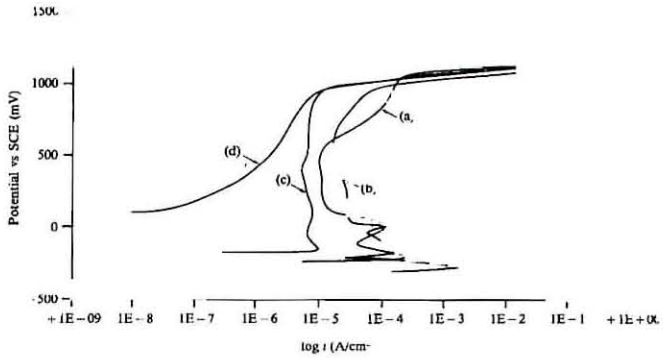

FIGURE 8. Anodic potentiodynamic scans of a 22% Cr duplex stainless steel with varying ruthenium contents in 20% H_2SO_4 at 55 °C. (a) 0% (b) 0,14% (c) 0,22% (d) 0,28% Ru

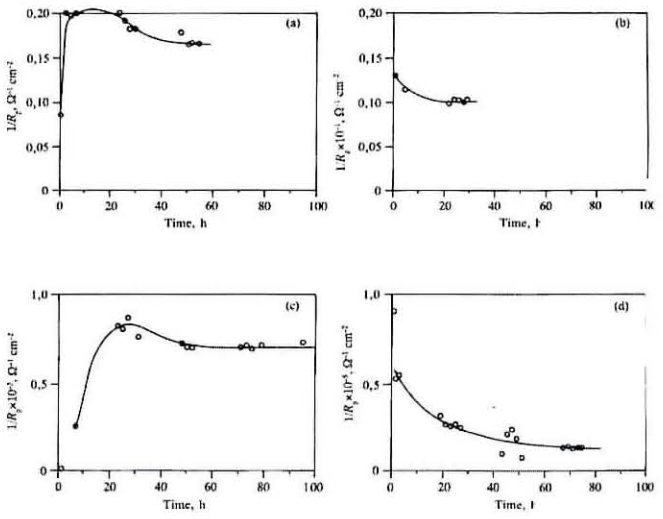

FIGURE 9. $1/R_p$ versus time responses for a 22% Cr duplex stainless steel with varying ruthenium contents in 20% H_2SO_4 at 55 °C. (a) 0% (b) 0,14% (c) 0,22% (d) 0,28% Ru

Figure 10 shows curves of open-circuit potential versus time for the alloys in 40 per cent sulphuric acid at 55 °C. The curves show that, in all cases, the stable open-circuit potential remained at largely electronegative values. This

implies that all four alloys were in a state of active dissolution, and should display active-to-passive transition behaviour upon polarization to noble potentials. This is also evident from their anodic potentiodynamic responses, given in Figure 11. The curves clearly show that there is no spontaneous passivation in any of the alloys. The cathodic potentiodynamic scans shown in Figure 12 indicate that ruthenium additions had little effect on cathodic Tafel characteristics. Differences in the experimental curves are associated mainly with differences in corrosion potential.

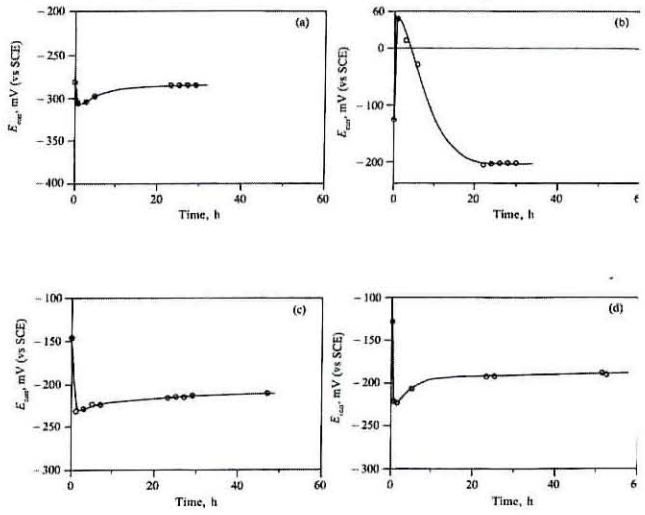

FIGURE 10. Open-circuit potential versus time responses for a 22% Cr duplex stainless steel with varying ruthenium contents in 40% H_2SO_4 at 55 °C. (a) 0% (b) 0.14% (c) 0,22% (d) 0,28% Ru

Table IV summarizes some electrochemical parameters for all four auoys. Tbese data reveal the following trends.

(a) An increase in the ruthenium content of the alloy resulted in an increase in the corrosion potential at a specific acid concentration.

(b) The passive current density, i_{pass}, increased as the acid concentration increased. The passive current density decreased significantly as the ruthenium content in the alloy increased. This implies that ruthenium has an inhibiting effect on the anodic dissolution of the alloy.

(c) The critical current density, i_{crit}, increased as the acid concentration increased, and decreased with increasing ruthenium content. The latter confirms the inhibition mentioned in (b) and proves that ruthenium inhibits the anodic dissolution of duplex stainless steels in sulphuric acid, as was also suggested by Higginson *et al.*[8] for a superferritic stainless steel containing ruthenium.

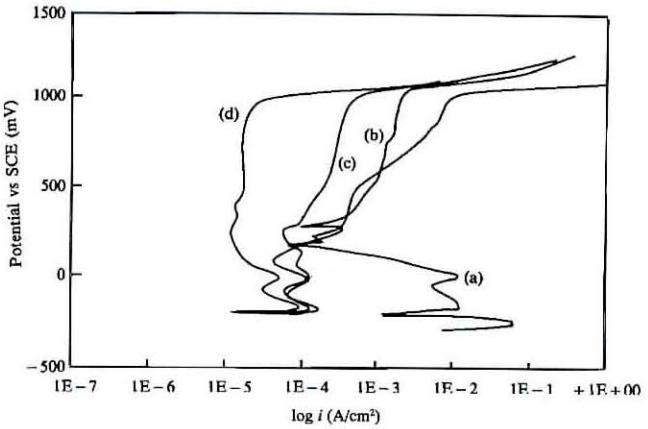

FIGURE 11. Anodic potentiodynamic scans of a 22% Cr duplex stainless steel with varying ruthenium contents in 40% H_2SO_4 at 55 °C. (a) 0% (b) 0.14% (c) 0,22% (d) 0,28% Ru

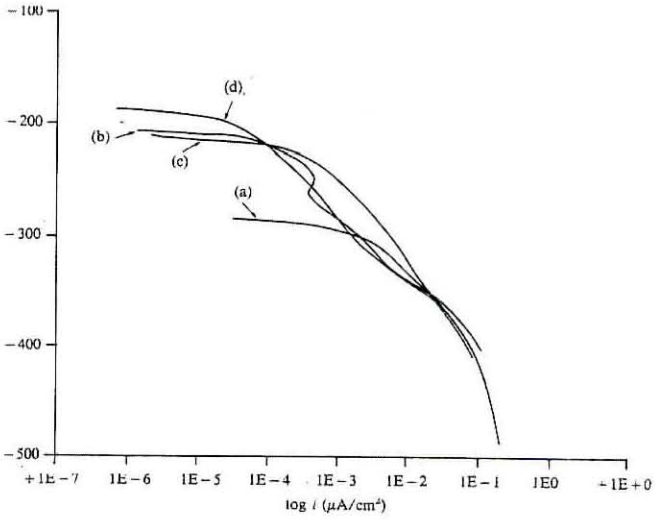

FIGURE 12. Cathodic potentiodynamic scans of a 22% Cr duplex stainless steel with varying ruthenium contents in 40% H_2SO_4 at 55 °C. (a) 0% (b) 0.14% (c) 0,22% (d) 0,28% Ru

It is well known that the presence of a PGM in an alloy promotes the hydrogen-evolution reaction and causes a shift in the corrosion potential to more noble values. However, the remarkable similarity of the cathodic potentiodynamic

TABLE IV

ELECTROCHEMCIAL PARAMETERS OBTAINED FROM POLARIZATION MEASUREMENTS FOR A 22% Cr DUPLEX STAINLESS STEEL WITH VARYING RUTHENIUM CONTENT IN H_2SO_4 AT 55 °C

	Steady state $1/R_p$ $\Omega^{-1}.cm^{-2}$			Steady state E_{corr} mV			i_{pass} A/cm²			i_{crit} A/cm²		
Alloy*	10%	20%	40%	10%	20%	40%	10%	20%	40%	10%	20%	40%
1	$5{,}0x10^{-4}$	$1{,}7x10^{-1}$	$1{,}6x10^{-2}$	-227	-295	-285	$4x10^{-6}$	$1x10^{-5}$	$2{,}5x10^{-3}$	$1{,}2x10^{-5}$	$1{,}8x10^{-3}$	$6x10^{-2}$
2	$6{,}9x10^{-4}$	$1{,}0x10^{-2}$	$4{,}9x10^{-3}$	-218	-249	-202	$3x10^{-6}$	$2x10^{-5}$	$1x10^{-3}$	$1{,}2x10^{-5}$	$2x10^{-4}$	$1{,}2x10^{-4}$
3	$8{,}1x10^{-7}$	$7{,}1x10^{-4}$	$1{,}1x10^{-2}$	+319	-167	-210	–	$7x10^{-6}$	$3x10^{-4}$	–	$1x10^{-5}$	$1{,}9x10^{-4}$
4	$9{,}8x10^{-6}$	$1{,}4x10^{-6}$	$2{,}0x10^{-3}$	+459	+100	-189	–	–	–	–	–	$9x10^{-5}$

* 1. Fe–22%Cr–9%Ni–3%Mo–0%Ru
2. Fe–22%Cr–9%Ni–3%Mo–0,14%Ru
3. Fe–22%Cr–9%Ni–3%Mo–0,22%Ru
4. Fe–22%Cr–9%Ni–3%Mo–0,28%Ru

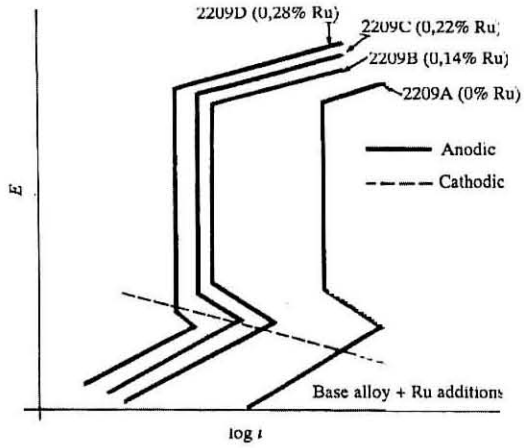

FIGURE 13. Schematic explanation of the effect of ruthenium on the polarization behaviour of 22% Cr duplex stainless steel in 20% H_2SO_4 at 55 °C

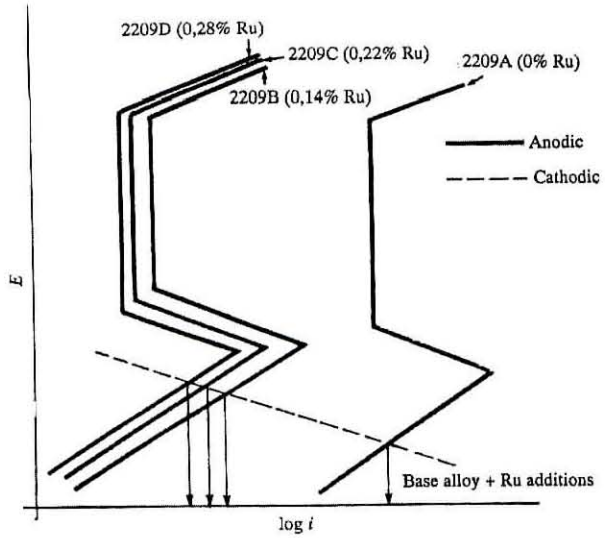

FIGURE 14. Schematic explanation of the effect of ruthenium on the corrosion behaviour of 22% Cr duplex stainless steel in 40% H_2SO_4 at 55 °C

curves in Figure 12 suggests that this mechanism does not apply in the case of ruthenium. Rather, the anodic corrosion characteristics in all three electrochemically investigated patterns can be explained solely on the basis that the ruthenium inhibited anodic dissolution.

The corrosion behaviour in 20 per cent sulphuric acid at 55 °C can therefore be explained diagrammatically by the Evans diagram in Figure 13. In this case only the alloy containing 0,28 per cent ruthenium passivated spontaneously. In 40 per cent sulphuric acid, the inhibition of anodic dissolution caused by the ruthenium additions becomes very clear, as is shown schematically in Figure 14. Although all the alloys investigated are in the active state, the corrosion rates of those containing ruthenium are two orders of magnitude smaller than the base alloy (Table III).

Conclusions

From the results of the mass-loss tests in acid solutions of different concentrations, four different corrosion behaviour patterns were distinguished.

In the first pattern, all the alloys passivate spontaneously and no detectable corrosion occurred. In the second pattern, the stainless steel without any ruthenium and the one containing 0,14 per cent ruthenium showed active–passive transition behaviour upon polarization while two of the alloys with sufficient amounts of ruthenium were in the passive state.

In the third pattern, a rise in the stable open-circuit corrosion potential was observed with an increasing ruthenium content in the alloy. Only the alloy with the highest ruthenium content was in a passive state. In the fourth pattern, all the alloys, regardless of their ruthenium content, were in the active state, with correspondingly high electronegative corrosion potentials.

The trends observed in the mass-loss tests were confirmed by the determined $1/R_p$ values. There was an increasc in $1/R_p$ values with an increase in the acid concentration, corresponding to an increase in the corrosion rate. Also evident was a decrease in $1/R_p$ values with an increase in the ruthenium content of the alloy, corresponding to a decrease in the corrosion rate.

It can be concluded that ruthenium increases the corrosion resistance by lowering the critical and passive current densities, thereby inhibiting anodic dissolution.

Acknowledgments

The authors gratefully acknowledge the contributions of Mr John Maskrey (casting and rolling of the alloys). Mrs I. Klingbiel (SEM and graphs), and Mrs M. Kincer (immersion tests). The valuable discussions and advice from Dr P.T. Wedepohl, Dr M.B. Cortie, Mr L.M. Matthews, aud Mr J. McEwan are also acknowledged. This paper is published by permission of Mintek.

References

1. Higginson, A. (1989). *Br. Corros. J.*, vol 24, p. 297.
2. McGill, I.R. (1990). *Plat. Met. Rev.*, vol 34, pp. 85, 144.
3 Potgieter, J.H. (1991). *J. Appl. Electrochem.*, vol. 21, p. 471.
4. Potgieter, J.H., Heyns, A.M., and Skinner, W. (1990). *J. Appl. Electrochem.*, vol. 20, p. 711.
5. Potgieter, J.H., and Cortie, M.B. (1990). *J.S. Afr. Inst. Min. Metall.*, vol. 90, p. 111.
6. ASTM. (1988). *Annual book of ASTM Standards.* vol. 03.02.
7 Dean, S.W. (1987). *Mater. Perf.*, Dec., p. 51.
8. Higginson, A., Newman, R.C. and Proctor R.P.M. (1989). *Corros. Sci.*, vol. 29, p. 1293.